

<http://ansinet.com/itj>

ITJ

ISSN 1812-5638

INFORMATION TECHNOLOGY JOURNAL

ANSI*net*

Asian Network for Scientific Information
308 Lasani Town, Sargodha Road, Faisalabad - Pakistan

Wavelet-based Total Variation Equation Image Restoration

¹Zhao Dong-Hong and ²Wang Chen-Chen

¹Department of Applied Mathematics, School of Mathematics and Physics Science,
University of Science and Technology Beijing, 100083, Beijing, People Republic of China

²Faculty of Science, University of Amsterdam, Netherlands

Abstract: In this study, we present an adaptive anisotropic diffusion total variation method which combine wavelet transformation and total variation (TV) equations. The algorithm puts high-frequency coefficients of wavelet into the iterative total variation equations to construct new wavelet coefficients. At the same time, we introduce spread function into this algorithm. In contrast with previous work combining TV restoration with wavelet compression, this method presented in this study not only treats the numerical solution in a novel way which decreases the computational cost associated with the solution of the TV model, but also introduces spread function into this algorithm, which adds the difficulties of the problem. We present a detailed description of our method which indicates that a combination of wavelet based on restoration technique with the TV model produces superior results.

Key words: Total variation equation, wavelet threshold method, image restoration technique, anisotropic diffusion

INTRODUCTION

The conventional image restoration model (Chan and Shen, 2000) deemed as an energy function of image uses partial differential equation which is based on Bayesian theory and variation problem and by minimizing the energy function the model restores the target region. In this study, we combine wavelets and TV partial differential equation image restoration techniques (Chan *et al.*, 2000) in a natural way to produce restoration results which have improved image quality and compression ratio compared to regular wavelet image restoration. The purpose of this study is to develop a fast method which combines TV restoration with wavelet compression, which is known to produce results which are superior to either method alone. In contrast with previous work (Shen and Chan, 2002) combining TV restoration with wavelet compression, the method presented in this study treats the numerical solution in a novel way which decreases the computational cost associated with the solution of the TV model.

Partial differential equation models (Scherzer, 1998) have been used in recent decades in image processing by solving the partial differential equation in the image domain. One of the most popular and successful

methodologies (Chambolle *et al.*, 1998) for image restoration is the Perona-Malik equation, which is based on the nonlinear version of heat equation:

$$u_t = \nabla \cdot [g(|\nabla u|) \nabla u]$$

In this model the thresholding function is small in regions of sharp gradients. A typical choice might be:

$$g(s) = \frac{1}{1 + \left(\frac{s}{k}\right)^2}$$

Since the image is considered as a continuous function (Rudin *et al.*, 1992), sharp edges and other 2-dimensional phenomena can be modeled into this equation through the application of concepts such as curvature and gradients.

This study is organized as follows: In section 2 we introduce wavelet-based TV image restoration model and indicate how wavelet coefficients may be used to generate sparse grids for use in numerical experiments involving the TV model. In section 3 we present results from several numerical experiments involving the TV model, wavelet-based image restoration and the wavelet

multilevel solution of the TV model. In section 4 we provide concluding remarks and give direction for future research.

WAVELET-BASED TV IMAGE DENOISING MODEL

This study is inspired by the P-M equation that introduces a diffusion coefficient function $c(\nabla f)$ to the TV method to guide the diffusion, which makes the diffusion implemented by different intensities in edges and gray scale flat areas. The literature (Aubert and Vese, 1997) proposed that the high-frequency part of wavelet reflects the gray change of point(x, y) of the image f. The places where changes in the gray-scale are small, the values of high frequency components are small; on the edge, the values of high-frequency components are larger. The three high-frequency components after wavelet transforming are cH (horizontal component), cV (vertical component) and cD (diagonal component).

Thus we define $M^2 = cH^2 + cV^2 + cD^2$, then the image use $c(M)$ instead of $c(\nabla f)$ to detect the edge.

Here use:

$$|\nabla f| \cdot \left(\frac{c(M)\nabla f}{|\nabla f|} \right)$$

to replace:

$$\nabla \cdot \left(\frac{\nabla f}{|\nabla f|} \right)$$

we get the new model:

$$f_i = |\nabla f| \nabla \cdot \left(\frac{c(M)\nabla f}{|\nabla f|} \right) - \lambda(f - f_0) \tag{1}$$

Equation 1 can be further written as:

$$\begin{aligned} f_i &= c(M)|\nabla f| \nabla \cdot \left(\frac{\nabla f}{|\nabla f|} \right) + |\nabla f| \nabla c(M) \frac{\nabla f}{|\nabla f|} \\ &\quad - \lambda(f - f_0) \\ &= c(M)|\nabla f| \nabla \cdot \left(\frac{\nabla f}{|\nabla f|} \right) + c'(M) \left(\frac{\partial M}{\partial x}, \frac{\partial M}{\partial y} \right) \\ &\quad (f_x, f_y) - \lambda(f - f_0) \\ &= c(M)|\nabla f| \nabla \cdot \left(\frac{\nabla f}{|\nabla f|} \right) + c'(M) \left(\frac{\partial M}{\partial x} f_x, \right. \\ &\quad \left. \frac{\partial M}{\partial y} f_y \right) - \lambda(f - f_0) \end{aligned} \tag{2}$$

Here, $c(M) = \exp(-M/k^2)$, k is a constant parameter. In our study, we take $k = 50$.

About (2), we can make the following explanation: In the first item, diffusion occurs only in the direction orthogonal to the gradient, while diffusion does not occur in the gradient direction, so that the edges of the image can be well maintained and even strengthened. And $c(M)$ controls the diffusion speed. When the point (x, y) is in the gray flat area, the value of $M(x, y)$ is relatively small, so $c(M)$ is relatively large, in this time the implementation of strong diffusion can remove isolated noise; When the point (x, y) at the edge of the image, it obtained local maximum $M(x, y)$, at this time the value of $c(M)$ is relatively small, so implementation of the diffusion will be weak, which will protect the important information. In the second item:

$$c'(M) \left(\frac{\partial M}{\partial x} f_x, \frac{\partial M}{\partial y} f_y \right)$$

controls transport speed, which is different in different directions: In the vertical direction at the edge, there is the largest transportation; while in the tangential direction, there is the smallest transportation. This item plays a very important role in maintaining the edge.

The third item is used to ensure that the processed image should approximate the original image. Here are the steps of using this model:

- For the initial noisy image f_0 , set the initial conditions: the time interval Δt , the number of iterations n, the gradient threshold k (where $k = 50$) and the regularization parameter λ . Set $f = f_0, n = 1$
- Select the appropriate wavelet, make the wavelet transformation and calculate M^n
- Calculate the n + 1 times images f^{n+1} and set $n = n+1$
- If $n \geq N$, then the algorithm terminates, at this time f_n is the finally denoised image

Otherwise, return to execute (ii)

EXPERIMENTS AND RESULTS

Image Toys: A is the original image; B is corrupted with additive white noise at a rate of 17.2929 PSNR; C is processed by TV algorithm for 50 times with $\lambda = 0.03, \Delta t = 0.2, h = 1$ and the result is at a rate of 21.8810 PSNR; D is processed by wavelet hard threshold method (Donoho and Johnstone, 1994) with wavelet'db3' and the result is at a rate of 25.1686 PSNR; E is processed by wavelet soft threshold method with wavelet'db3', and the result is at a rate of 25.1645 PSNR; F is processed by our new algorithm for 5 times with wavelet'db3', $\Delta t = 0.2, h = 1$, and the result is at a rate of 22.6923 PSNR; as the image toys are represented in Fig. 1 and Table 1.

Table 1: Image toys

Image	TV method	Wavelet hard threshold method	Wavelet soft threshold method	Our new algorithm
lena				
Iterations	50	-	-	5
Wavelet	-	db3	Db3	db3
PSNR	21.8810	25.1645	25.1686	22.6923
Time	1.712811s	2.060033s	2.060435s	1.173902

Table 2: Image lena

Image	TVmethod	Wavelet hard threshold method	Wavelet soft threshold method	Our new algorithm
lena				
Iterations	50	-	-	5
Wavelet	-	db4	db4	db4
PSNR	21.3718	22.2705	22.2915	22.8188
Time	7.655788s	5.260951s	5.280432s	2.969510s

Table 3: Image woman

Image	TVmethod	Wavelet hard threshold method	Wavelet soft threshold method	Our new algorithm
woman				
Iterations	50	-	-	5
Wavelet	-	db6	db6	db6
PSNR	22.0630	21.1083	21.1362	22.2098
Time	4.081018s	3.071091s	3.196478s	2.196478s

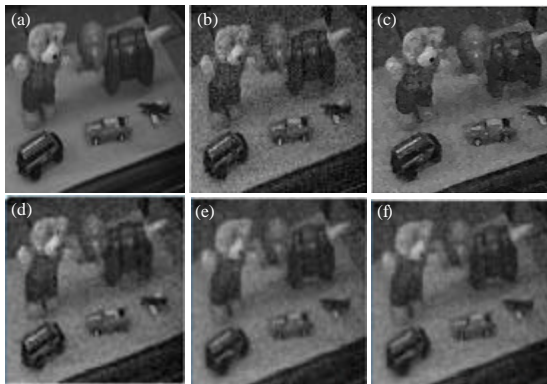


Fig. 1(a-f): Image TOYS

A is the original image; B is corrupted with additive white noise at a rate of 17.1825 PSNR; C is processed by TV algorithm for 50 times with $\lambda = 0.05$, $\Delta t = 0.2$, $h = 1$, and the result is at a rate of 21.3718 PSNR; D is processed by wavelet hard threshold method with wavelet'db4', and the result is at a rate of 22.2705 PSNR; E is processed by wavelet soft threshold method with wavelet'db4' and the result is at a rate of 22.2915 PSNR; F is processed by our new algorithm for 5 times with wavelet'db4' , $\Delta t = 0.2$, $h = 1$ and the result is at a rate of 22.8188 PSNR; as shown in Fig. 2 and Table 2.

A is the original image; B is corrupted with additive white noise at a rate of 17.6174 PSNR; C is processed by TV algorithm for 50 times with $\lambda = 0.028$, $\Delta t = 0.2$, $h = 1$, and the result is at a rate of 22.0630 PSNR; D is processed by wavelet hard threshold method with wavelet'db6' and the result is at a rate of 21.1083 PSNR; E is processed by wavelet soft threshold method with



Fig. 2(a-f): Image Lena



Fig. 3(a-f): Woman Image

wavelet'db6', and the result is at a rate of 21.1362 PSNR; F is processed by our new algorithm for 5 times with wavelet'db6' , $\Delta t = 0.2$, $h = 1$ and the result is at a rate of 22.2098 PSNR; images are represented in Fig. 3 and results are computed in Table 3.

CONCLUSION

This article introduces one new kind of methods which is the combination of wavelet threshold method and TV restoration method. From the experimental result, the amount of calculation in this method is small, so the speed is very fast. But the effect of this method with 5 iterations is better than the effect of TV restoration method with 50 iterations.

For this kind of combination methods, we have some follow-up works to do. The selection of the wavelet need to be further studied and whether this approach can be applied to other image restoration equation need to be tested. Our follow-up works are how to measure it to get the best restoration effect.

ACKNOWLEDGMENT

This study was supported by the Fundamental Research Funds for the Central Universities of University of Science and Technology of Beijing under Grant No.06108041.

REFERENCES

- Aubert, G. and L. Vese, 1997. A variational method in image recovery. *SIAM J. Numeric. Anal.*, 34: 1948-1979.
- Chambolle, A., R.A. De Vore, N.Y. Lee and B.J. Lucier, 1998. Nonlinear wavelet image processing: Variational problems, compression and noise removal through wavelet shrinkage. *IEEE Trans. Image Process.*, 7: 319-335.
- Chan, T., A. Marquina and P. Mulet, 2000. High-order total variation-based image restoration. *SIAM J. Scientific Comput.*, 22: 503-516.
- Chan, T.F. and J. Shen, 2000. Variational restoration of non-flat image features: Models and algorithms. *SIAM J. Applied Math.*, 61: 1338-1361.
- Donoho, D.L. and I.M. Johnstone, 1994. Ideal spatial adaptation by wavelet shrinkage. *Biometrika*, 81: 425-455.
- Rudin, L.I., S. Osher and E. Fatemi, 1992. Nonlinear total variation based noise removal algorithms. *Physica D Nonlinear Phenomena*, 60: 259-268.
- Scherzer, O., 1998. Denoising with higher order derivatives of bounded variation and an application to parameter estimation. *Computing*, 60: 1-27.
- Shen, J. and T.F. Chan, 2002. Mathematical models for local nontexture inpaintings. *SIAM J. Applied Math.*, 62: 1019-1043.